

## H passivation of shallow acceptors in Si studied by use of the perturbed- $\gamma\gamma$ -angular-correlation technique

H. Skudlik, M. Deicher, R. Keller, R. Magerle, W. Pfeiffer, P. Pross, and E. Recknagel  
*Fakultät für Physik, Universität Konstanz, D-7750 Konstanz, Federal Republic of Germany*

Th. Wichert

*Technische Physik, Universität des Saarlandes, D-6600 Saarbrücken, Federal Republic of Germany*

(Received 23 September 1991)

With the radioactive probe atom  $^{111}\text{In}$  as a representative for shallow acceptors in Si the passivation of acceptors by H was studied by using the perturbed- $\gamma\gamma$ -angular-correlation technique. It is shown that during passivation, close In-H pairs are formed and that the number of pairs exactly accounts for the number of deactivated acceptors. The formation of In-H pairs was investigated with use of different hydrogenation techniques and the stability of acceptor-H pairs was studied in isochronal annealing experiments.

### I. INTRODUCTION

In Si the passivation of shallow acceptors by H atoms, labeling the electrical deactivation of acceptor atoms by the formation of acceptor-H complexes, was discovered several years ago and stimulated a large number of experimental and theoretical studies. Sah, Sun, and Tzou<sup>1</sup> noticed the deactivation of B dopants in their metal-oxide semiconductor (MOS) capacitors and proposed the formation of electrically inactive B-H pairs to be responsible for this process. The H stemmed from the oxide layer of the device and was introduced in the bulk by avalanche injection of carriers. In *p*-type Si, spreading resistance measurements showed a superficial resistivity increase after exposure of B-, Al-, Ga-, and In-doped samples to a H plasma that reached several micrometers in depth.<sup>2,3</sup> Meanwhile, it is known that the deactivation of electrically active centers in semiconductors by H is a quite common phenomenon. It is observed for acceptors, donors, and deep levels in elemental and III-V semiconductors.<sup>4-8</sup> The change of electrical properties by H can rather easily unintentionally happen during common processing steps such as cleaning and etching in aqueous solutions,<sup>9</sup> plasma etching,<sup>2</sup> in devices under certain bias conditions,<sup>10</sup> and even just by air humidity.<sup>11</sup> A thorough study of the H passivation process is necessary in order to avoid unwanted alterations of material properties but also to use it for possible device tuning applications.

A variety of experimental techniques has contributed to the knowledge on the H passivation of shallow (group-III) acceptors in Si. Corresponding to their sensitivities, they work in quite different concentration regimes, which should be considered when the results are compared. Evidence for a formation of acceptor-H pairs being responsible for the acceptor deactivation came from secondary-ion-mass spectroscopy (SIMS) measurements, which revealed a quantitative correlation between the B and D concentrations in a B-doped Si sample treat-

ed in a D plasma.<sup>12</sup> Infrared<sup>13-15</sup> (IR) and Raman spectroscopy<sup>16</sup> proved that during H plasma treatments microscopic complexes are formed. Isotopical exchange ( $^1\text{H}$ ,  $^2\text{D}$  and  $^{10}\text{B}$ ,  $^{11}\text{B}$ ) showed that H and B atoms were involved in the complexes which were identified via their vibrational absorption spectra.<sup>17</sup> However, there are several difficulties: The dopant concentrations, in the range of  $10^{18}$ – $10^{19}$   $\text{cm}^{-3}$ , used in these experiments do not allow the investigation of contamination pathways which are relevant at much lower concentrations. The investigation of the acceptor In is not possible because of its too-low solubility. In IR and Raman experiments the absolute fraction of acceptor atoms involved in acceptor-H pairs is difficult to quantify.

The lattice site of H was investigated experimentally by ion channeling<sup>18-20</sup> and discussed in numerous theoretical studies (e.g., Refs. 21–29) for B-doped Si converging to a H site situated on or close to a bond between the B acceptor and a neighboring Si atom. Methods observing the electronic properties of semiconductors like the above-mentioned spreading resistance technique are, by far, more sensitive. They measure integral electrical properties resulting from the complex formation, but do not supply direct information on the microscopic properties and chemical constituents of the complexes. In B-doped Si treated in a H plasma, Hall measurements proved a reduction of the free-hole concentration paralleled by an increase of the hole mobility, suggesting the removal of B<sup>-</sup> scattering centers by the formation of neutral B-H pairs.<sup>30</sup> The electrically active acceptor concentration was also measured by capacitance-voltage (*C-V*) profiling and was modified by the applied bias.<sup>10,31,32</sup> By photoluminescence the removal of acceptor levels from the band gap as a result of H treatments was observed.<sup>33</sup>

Continuing earlier studies of the H passivation,<sup>34-36</sup> in this work the microscopically sensitive perturbed- $\gamma\gamma$ -angular-correlation technique (PAC) has been applied using the radioactive probe atom  $^{111}\text{In}$ . The behavior of the PAC signal of  $^{111}\text{In}$ -H pairs, which is influenced by the

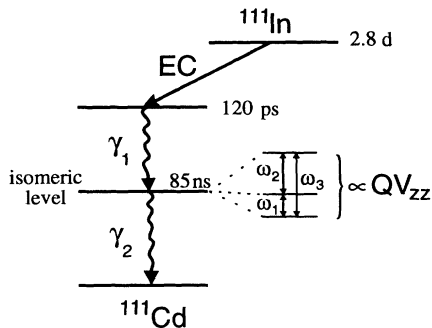


FIG. 1. Decay scheme of the PAC probe atom  $^{111}\text{In}$  which converts to  $^{111}\text{Cd}$  via electron capture (EC). The half-lives of the excited states are indicated. The nuclear splitting of the isomeric level, which is used in the PAC measurement, is shown for the case of an axially symmetric EFG.

chemical transmutation of the probe atom  $^{111}\text{In}$  to  $^{111}\text{Cd}$  (see Fig. 1) was described recently.<sup>37,38</sup> The study of the acceptor In is complementary to IR and Raman studies. Using PAC the absolute number of In-H pairs can easily be quantified and acceptor concentrations below  $10^{17} \text{ cm}^{-3}$  can be studied, which are comparable to those used by electrical techniques, like  $C$ - $V$  profiling or the Hall effect. After the description of the technique and the experimental details in Secs. II and III, respectively, the experimental results are presented in Sec. IV. They comprise the identification of In-H pairs formed during H passivation of In-doped Si. Furthermore, the correlation between electrical deactivation and acceptor-H pair formation is investigated to clarify the question whether every deactivated acceptor atom is involved in an acceptor-H pair; this opinion is commonly accepted, but not strictly proven, up to now. Finally, contamination pathways are identified and the efficiency of low-energy  $\text{H}^+$  implantations as well as the thermal stability of the In-H pairs are investigated. In Secs. V and VI these data are discussed and summarized.

## II. METHOD

The perturbed- $\gamma\gamma$ -angular-correlation technique has recently been described.<sup>39</sup> Therefore only a brief introduction will be given here. PAC uses radioactive probe atoms whose decay involves a  $\gamma\gamma$  cascade, in this case  $^{111}\text{In}$  (Fig. 1). With a half-life of 2.8 days, it decays via electron capture to an excited state of  $^{111}\text{Cd}$ . Then, two  $\gamma$  transitions populate and depopulate an isomeric nuclear level and lead to the stable ground state of  $^{111}\text{Cd}$ . The hyperfine interaction between the nuclear quadrupole moment  $Q$  and the electric-field gradient (EFG), characteristic for the charge distribution in the immediate environment of the probe nucleus, causes a splitting of the isomeric level whose half-life is 85 ns. By a standard four detector setup (Fig. 2) the correlation in space and time between the two  $\gamma$  quanta arising from the same  $^{111}\text{In}$  decay is detected. For all 12 possible combinations of detectors the time elapsed between the first and second

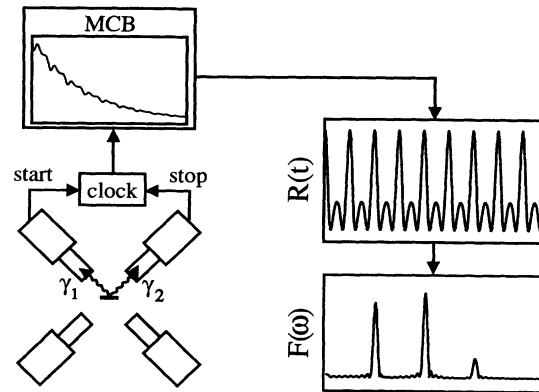


FIG. 2. Schematic block diagram of a PAC measurement with four  $\gamma$  detectors. Using the  $\gamma_1$  and  $\gamma_2$  radiation from the same decay event to start and stop a clock, respectively, separate time spectra are collected in a multichannel buffer (MCB) for every detector combination. The resulting 12 spectra are combined into a single  $R(t)$  spectrum whose Fourier transform shows the three frequencies  $\omega_n$ ,  $n = 1, 2, 3$ , associated with each EFG.

$\gamma$  transitions is measured and stored. The resulting time spectra are combined into a single  $R(t)$  spectrum which contains the information about the hyperfine interaction of the probe nucleus with the electromagnetic fields of its environment.  $R(t)$  is described by

$$R(t) = A \sum_i f_i G_i(t). \quad (1)$$

The perturbation factor  $G(t)$  comprises the transition frequencies  $\omega_n$  of the split isomeric level and reads, in the case of a pure electric quadrupolar interaction,

$$G(t) = S_0 + \sum_{n=1}^3 S_n \cos(\omega_n t). \quad (2)$$

The anisotropy  $A$  is a nuclear parameter of the  $\gamma\gamma$  decay folded with the angular resolution of the setup and equals  $-0.130$  in the present experiments. Different fractions of probe atoms  $f_i$  ( $\sum_i f_i = 1$ ) can be exposed to different EFG's with strengths  $V_{zz}^i$  (largest component of the traceless EFG tensor). The EFG is described through the quadrupole coupling constant  $\nu_Q = eQV_{zz}/h$ . Because of the  $\frac{5}{2}$  spin of the isomeric state for each EFG three transition frequencies  $\omega_n$  occur in the spectrum, which are  $\omega_n = n(3\pi/10)\nu_Q$  for axial symmetry of the EFG tensor ( $V_{xx} = V_{yy}$ ). The amplitudes  $S_n$  depend on the orientation of the principal axes system of the EFG with respect to the detector system and they are reduced by the finite angular and time resolution of the setup.

For an In atom, substitutionally incorporated in the Si lattice, the EFG vanishes because of the tetrahedral symmetry of the electrical charge distribution and therefore the  $R(t)$  spectrum becomes time independent [ $G(t) = 1$ ]. If the probe atoms are exposed to a well-defined EFG pronounced oscillations occur in the  $R(t)$  spectrum and the corresponding peaks of  $\omega_n$  appear in the Fourier transform  $F(\omega)$  (see Fig. 2). Such a well-defined EFG is

generated by trapping a defect at the probe atom in a unique configuration. From a fit of the theoretical function (1) to the experimental  $R(t)$  spectrum, the absolute fractions  $f_i$  (with a detection limit of about 1%), the quadrupole coupling constants  $\nu_Q$ , and the amplitudes  $S_n$  are determined.

The  $\gamma$  rays recorded in the PAC experiment are emitted by the residual isotope  $^{111}\text{Cd}$  when the original In-defect complex has converted to a Cd-defect complex. Thus the symmetry and orientation observed are, strictly speaking, that of the residual complex containing Cd, which is not necessarily identical to that of the initial In-defect complex. Questions concerning this chemical transmutation and associated relaxation effects are discussed in detail elsewhere.<sup>37,38</sup>

The coupling constant  $\nu_Q$  serves as a characteristic pattern and allows the reliable recognition of a once tagged complex under all experimental circumstances. The amplitude  $f$  of the modulation corresponds to the fraction of probe atoms involved in the complex and is a quantitative measure of how many complexes have been formed. Using its characteristic pattern  $\nu_{Qi}$  a complex can be identified by varying the experimental conditions and the fraction  $f_i$  allows the investigation of its formation and dissociation.

### III. EXPERIMENTAL DETAILS

We used  $p$ -type Si, homogeneously doped with B at different levels. For B concentrations below  $10^{15}\text{ cm}^{-3}$  the samples are referred to as “intrinsic.” The typical depth concentration profiles of a sample are displayed in Fig. 3. The radioactive  $^{111}\text{In}$  probe atoms were implanted at room temperature, usually with 350 keV and sometimes with 60 keV. The implantation depths are  $1640\pm 470$  and  $370\pm 120$  Å and the peak concentrations are  $5\times 10^{16}$  and  $2\times 10^{17}\text{ cm}^{-3}$ , respectively. In some experiments the resistivity of the samples was measured parallel to the PAC measurement with a four-point

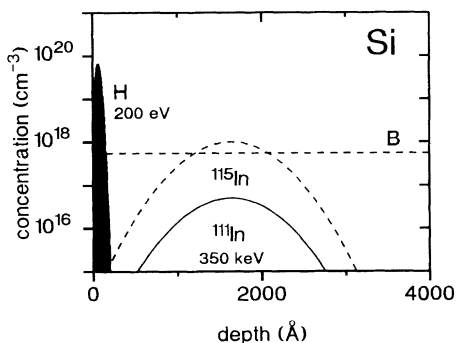


FIG. 3. Depth profiles of impurity concentrations for typical samples: The  $^{111}\text{In}$  probe atoms are implanted at 350 keV (solid line). H loading with 200-eV implantation energy (here,  $5\times 10^{13}\text{ cm}^{-2}$ ) leads to a shallow H profile (black) so that H has to diffuse into the sample to form In-H pairs. Several experiments were performed using higher  $p$ -type doped material (dashed lines), e.g., either homogeneous B-doped (here,  $5.5\times 10^{17}\text{ cm}^{-3}$ ) or additionally implanted with stable  $^{115}\text{In}$  (peak concentration  $10^{18}\text{ cm}^{-3}$ ).

probe. In these cases a special sample design was required because the conductance caused by the typically  $5\times 10^{11}\text{ cm}^{-2}$  radioactive  $^{111}\text{In}$  atoms is much too low to be detected. Therefore an additional doping by implantation of stable  $^{115}\text{In}$  acceptor atoms was performed. For damage recovery and electrical activation the implants were annealed at 1173 K under flowing  $\text{N}_2$  gas either for 20 s in a rapid thermal annealing setup (RTA) or for 10 min in a resistance heated furnace. Loading of the Si samples with H was achieved in a H plasma, in darkness in hot  $\text{H}_2\text{O}$  (353–373 K), or quantitatively controlled by means of a low-energy implantor (Colutron corporation) at 200 eV, allowing an element-specific and almost-defect-free doping. According to a Monte Carlo simulation<sup>40</sup> of the 200-eV implantation, 16% of the  $\text{H}^+$  ions are backscattered from the Si lattice, the remaining ions are deposited in a depth of  $65\pm 30$  Å, and less than 0.5 vacancies are created per implanted ion. For the study of the thermal stability of the In-H pairs the annealing was performed in air up to 523 K and in a furnace under flowing  $\text{N}_2$  above this temperature.

### IV. RESULTS

To investigate whether a possible acceptor-H complex formation is the reason for the acceptor deactivation in H-loaded Si, an intrinsic Si sample was doped with  $^{111}\text{In}$  and exposed to a H plasma (15 min, 13.56 MHz, 320 V, 0.6 mbar). In Fig. 4(a) the PAC spectrum taken from this sample at 300 K is shown. It exhibits pronounced oscillations proving that well-defined complexes have been formed with the  $^{111}\text{In}$  probe atoms. The Fourier transform indicates that two EFG's are observed, labeled by their coupling constants  $\nu_{Q1/-} = 349$  MHz and  $\nu_{Q2} = 463$  MHz. The identical EFG's are observed in samples loaded with H in  $\text{H}_2\text{O}$  [353 K, 100 min; Fig. 4(b)] or implanted with low energetic  $\text{H}^+$  ions [200 eV,  $10^{14}\text{ cm}^{-2}$ ; Fig. 4(c)]. This result is characteristic for intrinsic samples. The same loading procedures applied to B-doped samples whose concentrations exceed the implanted local  $^{111}\text{In}$  concentration always lead to the observation of a coupling constant  $\nu_{Q1}$  whose value ranges from  $\nu_{Q1/0} = 269$  MHz to  $\nu_{Q1/-} = 349$  MHz at 300 K and strictly depends on the electrically active B concentration in the sample. An example is shown in Fig. 4(d) for a B concentration of  $5.5\times 10^{17}\text{ cm}^{-3}$ , where  $\nu_{Q1} = 311$  MHz is observed after  $\text{H}^+$  implantation and annealing at  $T_A = 410$  K. From the amplitude of the modulation the fraction of probe atoms forming complexes is extracted. It varies between 15% and 45% in the spectra shown in Fig. 4. All EFG's observed after H loading are axially symmetric along  $\langle 111 \rangle$  lattice directions.<sup>38</sup> The designations of the observed coupling constants  $\nu_{Q1}$  and  $\nu_{Q2}$  refer to two different configurations of the  $^{111}\text{Cd}$ -H complex generated by the chemical transmutation of the  $^{111}\text{In}$  probe atom, whereby the first configuration can occur in different charge states  $(\text{Cd-H})^{-w}$  with  $0 \leq w \leq 1$ . The population of the different structural and electronic states in dependence on the electronic conditions in the sample is well known<sup>38</sup> and will be used for the discussion of the experiments.

In order to establish a quantitative correlation between the number of formed In-H complexes and the number of deactivated In acceptor atoms in addition to the fraction of complexes the change in electrical conductivity has to be known. For this purpose four-point resistivity measurements were performed parallel to the PAC experiment. Because the number of implanted radioactive  $^{111}\text{In}$  atoms (about  $5 \times 10^{11} \text{ cm}^{-2}$ ) is too small to produce a detectable conductance, stable  $^{115}\text{In}$  was additionally implanted at the 20 times higher dose of  $10^{13} \text{ cm}^{-2}$  with the same energy of 350 keV increasing the peak concentration to  $10^{18} \text{ cm}^{-3}$ . After activation of the implant by rapid thermal annealing at 1173 K the sample was post annealed for 10 min at 630 K prior to the low-energy  $\text{H}^+$  implantation (200 eV) at 400 K with a dose of  $5 \times 10^{13} \text{ cm}^{-2}$ . This procedure should prevent electrical alterations of the sample during the subsequent low-temperature annealing (400–625 K) due to effects other than the interaction between H and the acceptor atoms. In Fig. 5(a) the fraction of probe atoms forming In-H complexes observed after H loading and during a subse-

quent isochronal annealing experiment is shown. In Fig. 5(b) the conductance of this sample (open circles) is plotted for comparison. In addition the data of reference samples are shown, which consisted of the same base material (B-doped,  $2000 \Omega \text{ cm}$ ) and were subjected to the same annealing treatments as the In-doped sample, but were not implanted with In or H. Their conductances vary between 0.11 and 0.20 mS (box). After H implantation, 53% of the In atoms have formed In-H complexes and the conductance decreases towards the values of the intrinsic reference samples. During annealing an increase of the number of complexes is always reflected by a decrease of the conductance and vice versa. Especially the dissolution of the In-H complexes starting above 525 K is accompanied by a recovery of the conductance to the value before H loading. A quantitative comparison of the PAC and conductance data is performed in Sec. V B. After this annealing sequence a second  $\text{H}^+$  implantation was performed with the high dose of  $10^{15} \text{ cm}^{-2}$  to investigate how many In-H complexes could be formed in this sample. This maximum fraction was determined to 78%

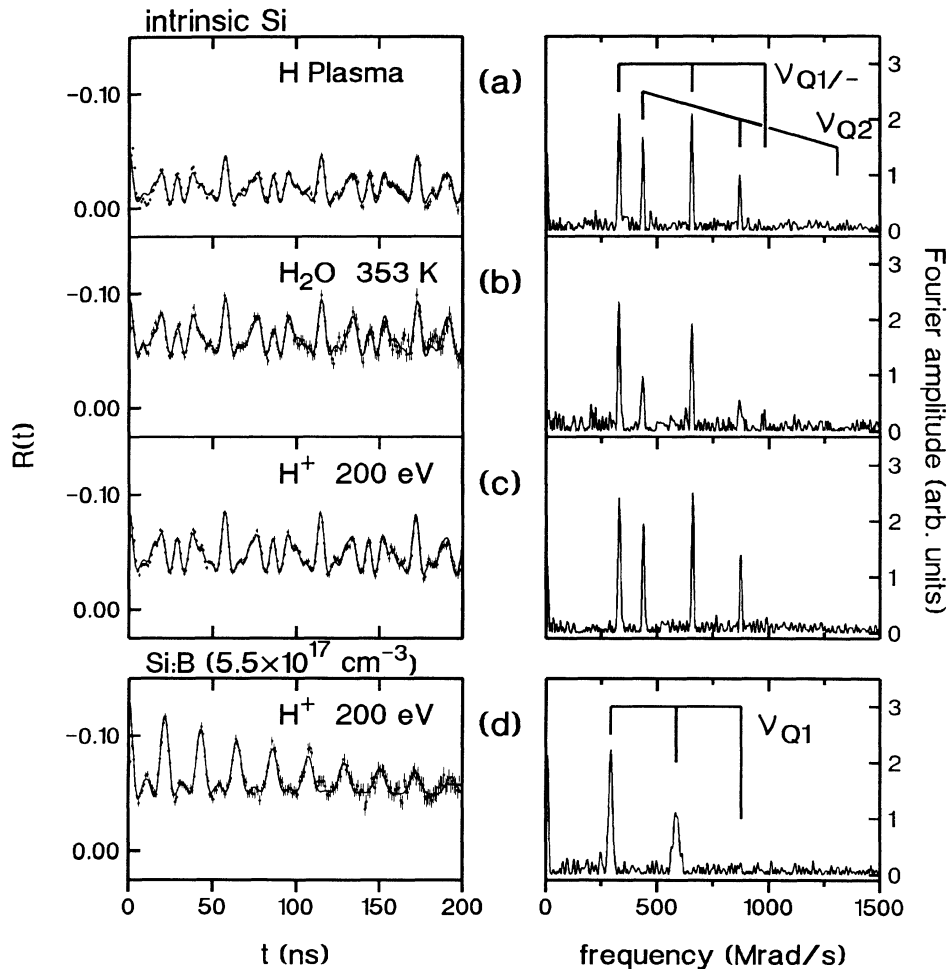


FIG. 4. PAC spectra (left) and their Fourier transforms (right) of H-loaded Si samples with different homogeneous B concentrations. In intrinsic Si after loading by (a) H plasma, (b) in hot  $\text{H}_2\text{O}$ , or (c) by low-energy  $\text{H}^+$  implantation the formed In-H pairs are characterized by  $\nu_{Q1/-} = 349 \text{ MHz}$  and  $\nu_{Q2} = 463 \text{ MHz}$  (at 300 K). In (d) higher B-doped Si,  $\nu_{Q1}$  assumes values between  $\nu_{Q1/0} = 269 \text{ MHz}$  and  $\nu_{Q1/-} = 349 \text{ MHz}$  (in this case 311 MHz at 300 K) depending on the B concentration, the degree of passivation, and the sample temperature (Ref. 38).

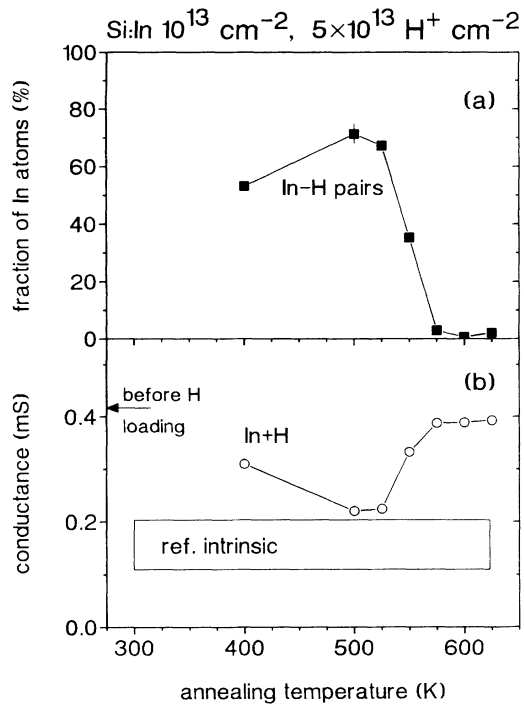


FIG. 5. Isochronal annealing experiment of an intrinsic Si sample implanted with  $^{111}\text{In}$  and  $^{115}\text{In}$  at 350 keV and loaded with H at 200 eV (a) Fraction of In atoms in In-H pairs (solid squares), and (b) conductance of the same sample (open circles). The conductance before H loading is marked by an arrow; the conductance range observed for rapid thermal annealed intrinsic reference samples is indicated by a box.

from the PAC spectrum shown in Fig. 6.

Using the known characteristic pattern of the In-H complexes their formation conditions can be easily pursued by PAC and even the unintentional contamination of a sample with H can reliably be identified. Some examples of procedures leading to the occurrence of the In-H specific coupling constants are given in Fig. 7. In (a), during the evaporation of Pd on top of  $^{111}\text{In}$  implanted and oxidized Si, used for the production of a MOS

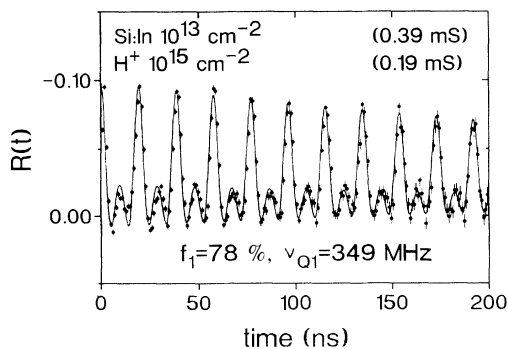


FIG. 6. PAC spectrum of the sample from Fig. 5 which was implanted with a high H dose after the annealing sequence. The conductance before and after  $\text{H}^+$  implantation, the fraction  $f_1$ , and coupling constant  $\nu_{Q1}$  of the In-H pairs are given.

structure, 8% of the radioactive probe atoms form In-H complexes as is visible by  $\nu_{Q1}$  in the PAC spectrum. In (b) low energetic Cu ions (200 eV,  $10^{14} \text{ cm}^{-2}$ ), being responsible for another passivation mechanism occurring during chemomechanical polishing of Si,<sup>41</sup> were implanted and the sample was measured at 78 K. Besides the formation of In-Cu complexes (marked in the Fourier transform) a small fraction of probe atoms (3%) has formed In-H complexes as is evidenced from the occurrence of  $\nu_{Q1/0}$ . The last spectrum (c) stems from a sample that was implanted with  $^{111}\text{In}$  (60 keV) and annealed for electrical activation. Storage of the sample for several hours in warm (about 320 K) and humid air decorated 50% of the In acceptors with H and led to the occurrence of  $\nu_{Q1/-}$  at ambient temperature.

The efficiency of In-H complex formation during low-energy  $\text{H}^+$  implantation was investigated in a sample doped by subsequent implantation of radioactive  $^{111}\text{In}$  and stable  $^{115}\text{In}$  ( $10^{13} \text{ cm}^{-2}$ ) with the same energy and activated in one annealing step. H was implanted with increasing dose at an energy of 200 eV and a temperature of 400 K, just below the dissociation temperature of the complexes (see below). The fraction of In-H complexes observed for different H doses is shown in Fig. 8(a) along with the conductance of the sample measured with a four-point probe [Fig. 8(b), open circles]. The first dose of  $5 \times 10^{12} \text{ cm}^{-2}$  results in a fraction of 9% complexes. Since the radioactive and the stable In are chemically identical this value means every fifth H atom has been trapped at an In atom. For higher doses the number of formed complexes saturates at about 65%. With increasing H dose, the conductance of the sample has decreased, indicating the deactivation of the In acceptor atoms. In Fig. 8(b), besides the conductance  $\sigma$ , the coupling constant  $\nu_{Q1}$  is plotted (solid squares), which is known to depend on the Fermi-level position in the sample.<sup>36-38</sup> The increase from 335 to 349 MHz during H loading indicates the increase of the Fermi level caused by the deactivation of the In acceptors.

When the  $\text{H}^+$  implantation energy is too high the efficiency of In-H pair formation is dramatically decreased. For an implantation energy of 1 keV the fraction of In-H pairs is about ten times smaller than for an energy of 200 eV.

From the study of the dissociation of In-H complexes during an isochronal annealing program under different experimental conditions, the stability of In-H complexes can be determined. As an example, in Fig. 9 the decrease of the modulation amplitude belonging to the In-H complexes is shown for increasing annealing temperature. The results presented below are summarized in Fig. 10. In intrinsic material (a) after deactivation in hot  $\text{H}_2\text{O}$  the In-H complexes abruptly disappear at a temperature of 420 K, whereas after low-energy  $\text{H}^+$  implantation the dissociation step is less sharp. The same annealing experiments performed in samples with homogeneous B concentrations exceeding the implanted  $^{111}\text{In}$  concentration show quite different results (b). For Si doped with  $1.6 \times 10^{17} \text{ B cm}^{-3}$ , first a marked increase instead of a decrease in the fraction of In-H complexes is observed around 380 K. The dissolution is delayed to much higher

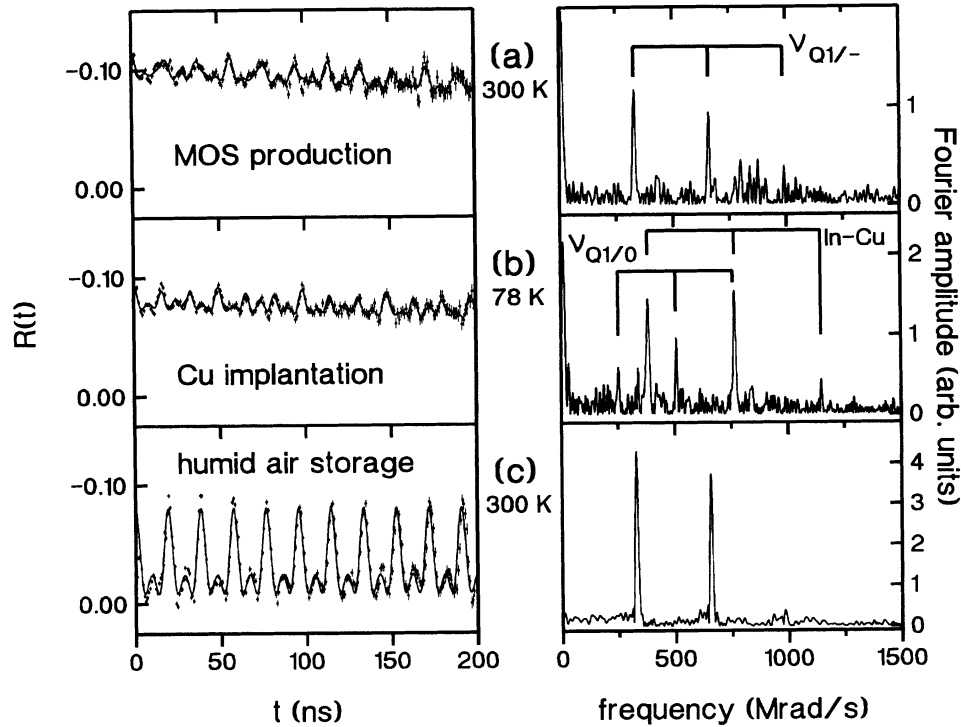


FIG. 7. PAC spectra (left) and their Fourier transforms (right) recorded at the indicated sample temperatures showing the unintentional formation of In-H pairs during the production of (a) a MOS structure, (b) 200-eV  $\text{Cu}^+$  implantation, and (c) storage in humid air. In (b) the small amount of In-H pairs can easily be detected in presence of the simultaneously formed In-Cu pairs.

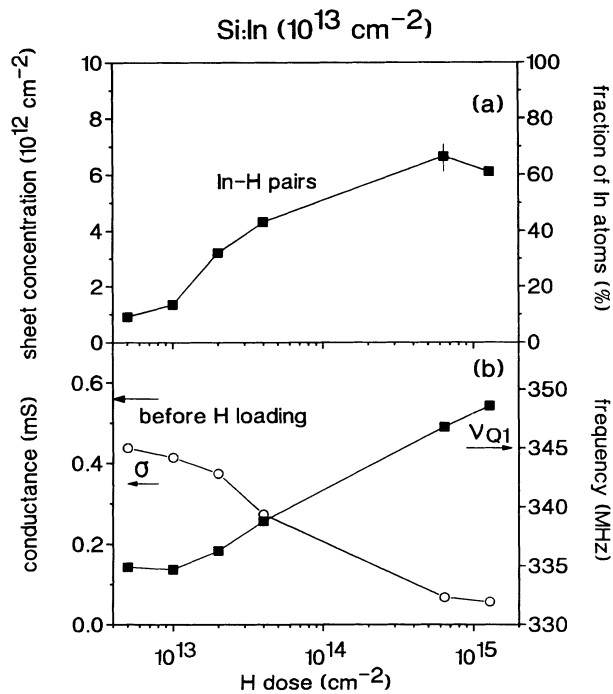


FIG. 8. (a) Fraction of In atoms in In-H pairs (right scale, solid squares) and, respectively, sheet concentration of In-H pairs (left scale) plotted against the H dose implanted in In-doped Si. (b) Conductance  $\sigma$  (left scale, open circles) and coupling constant  $\nu_{Q1}$  (right scale, solid squares) observed at the same sample. The conductance prior to H implantation is indicated.

temperatures above 500 K. The same behavior is observed at samples with even higher B concentrations. To investigate this codoping related increase for another acceptor species an intrinsic sample was implanted with Ga in addition to the radioactive  $^{111}\text{In}$  (c). The implantation was performed at two different energies of 155 and 310

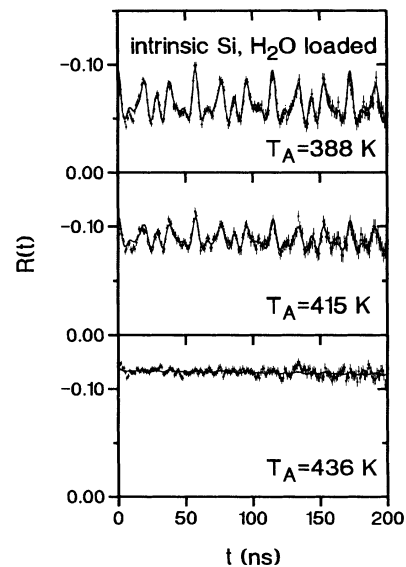


FIG. 9. PAC spectra recorded at an intrinsic Si sample loaded in hot  $\text{H}_2\text{O}$  (353 K, 100 min) after isochronal annealing at different temperatures  $T_A$ . The decay of the fraction of In-H pairs in this experiment is shown in Fig. 10(a).

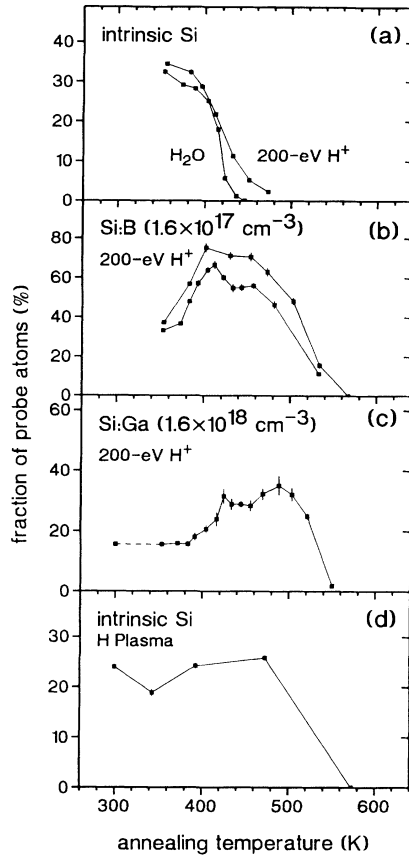


FIG. 10. Fractions of  $^{111}\text{In}$  atoms in In-H pairs vs isochronal annealing temperature for (a) and (d) intrinsic, (b) B-doped, and (c) Ga-doped Si loaded with H by different techniques.

keV to produce an almost homogeneous Ga concentration of  $1.6 \times 10^{18} \text{ cm}^{-3}$  between 900 and 2400 Å. Now the increase in the fraction of In-H complexes occurs around 400 K, which is above the temperature observed for B and below the dissociation temperature for In-H complexes observed in intrinsic samples. The stability of the complexes was also studied after hydrogenation of an intrinsic sample in a H plasma (d). In this case the fraction of In-H complexes persists to significantly higher temperatures compared with the samples shown in Fig. 10(a) and the dissociation takes place around 500 K.

## V. DISCUSSION

### A. Identification of In-H pairs in Si

The results of Fig. 4 prove that the identical In-H pairs are formed during the different hydrogenation treatments: The identical well-defined EFG's, characterized by  $\nu_{Q1/-}$  and  $\nu_{Q2}$ , are observed in intrinsic samples after loading in a H plasma, H<sub>2</sub>O, or by low H<sup>+</sup> energy implantation. Because no or very few intrinsic defects are created in case of the H<sub>2</sub>O treatment and of the low-energy implantation, complexes formed between In and intrinsic defects can be ruled out. Because of the mass selected implantation nothing but H was introduced into

the sample verifying that H has been trapped at the  $^{111}\text{In}$  probe atoms. It has been shown<sup>38</sup> that the different occurring EFG's correspond to different states of the  $^{111}\text{Cd}$ -H complexes produced by the radioactive decay of  $^{111}\text{In}$  to  $^{111}\text{Cd}$ . Their occurrence and population depend on species and electrically active concentration of acceptors and on the temperature and can be reversibly varied by changing electronic parameters that cannot effect, however, a change of the composition of the complex. Therefore the occurrence of different EFG's is not caused by different number of H atoms trapped at the In. That means only one stoichiometry of In-H complexes is formed under all experimental conditions, which is most probably an In-H pair. This conclusion is supported by the observation of axial symmetry along  $\langle 111 \rangle$  axes of the Si lattice for all Cd-H complexes,<sup>38</sup> measured after the decay of  $^{111}\text{In}$  to  $^{111}\text{Cd}$ , which can hardly be explained by more than one H atom involved in the complex. This finding extends the experimental evidence for acceptor-H pairing in Si after hydrogenation to the acceptor In, which already existed for B-H, Al-H, and Ga-H pairs identified by IR (Refs. 13–15) and Raman studies.<sup>16</sup>

### B. Correlation of pair formation and deactivation

Although a substantial fraction of acceptor atoms has formed complexes after a H treatment known to deactivate the dopants, it is not obvious that the complex formation is responsible for the deactivation. The term H passivation means that the formation of an acceptor-H pair renders the acceptor atom electrically inactive. If this is true, the number of formed acceptor-H pairs has to be equal to the number of deactivated acceptors at any time of the experiment. The establishment of this correlation requires the combination of a method capable of determining quantitatively the number of formed pairs with quantitative electrical measurements. For B-doped Si, combined SIMS and spreading resistance measurements<sup>14,42</sup> have shown the correlation between the concentration of deuterium and the concentration of active acceptors. For high acceptor densities, the deuterium and the acceptor concentrations converge.<sup>14</sup> But there is no direct information on the formation of close acceptor-H pairs available in these measurements. For the acceptor In the number of In-H pairs formed is easily to quantify by PAC: The fraction of  $^{111}\text{In}$  atoms involved in an In-H pair is a direct result of the measurement. This fraction multiplied with the dose of implanted In atoms, radioactive  $^{111}\text{In}$  and stable  $^{115}\text{In}$ , which chemically behave equal, gives the sheet concentration of In-H pairs formed. The concentrations of In-H pairs calculated in this way from the experimental data in Fig. 5(a) are shown in Fig. 12.

For a comparison the four-point resistivity data from the same experiment [Fig. 5(b)] have to be converted to absolute numbers of electrically active In atoms. Because for Si, little information is available in the literature about the relationship between the measured resistivity and the In concentration we adapted the B resistivity-concentration standard curve<sup>43</sup> for In (Fig. 11). The identical concentration of ionized acceptors corresponding to

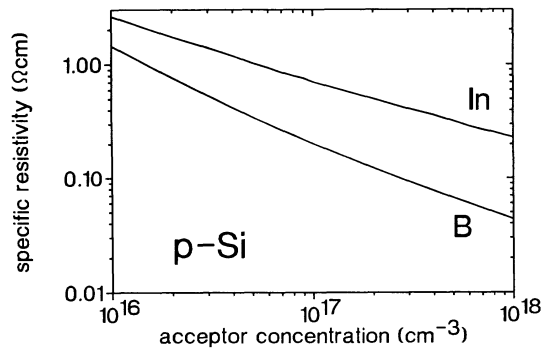


FIG. 11. Dependence of the resistivity of *p*-type Si on the acceptor concentration. The curve for In has been calculated from the B standard curve (Ref. 43).

equal concentrations of free holes was assumed to generate the same conductivity for B and In doping. This takes into account the influence of the concentration but not of the species of the ionized acceptors on the hole mobility. Therefore the resistivity versus concentration curve for In in Fig. 11 bears the same uncertainty as that for B, on which it is based. The uncertainty may be increased by a possible influence of the In dopants on the mobility of the carriers due to the size differences between In and B. The result basically agrees with that of Sclar<sup>44</sup> obtained by similar calculations.

The Gaussian-shaped In profile ( $1640 \pm 470$  Å) was approximated by a rectangular one with a width of 1250 Å corresponding to an averaged absolute concentration of  $8 \times 10^{17}$  In  $\text{cm}^{-3}$ . The rapid thermal anneal at 1173 K for 20 s creates a small bulk conductance in our intrinsic base material, reducing its resistivity from 2000 Ω cm to values between 650 and 1300 Ω cm. This effect contributes an offset conductance, scattering between 0.11 and 0.20 mS for unimplanted and annealed intrinsic reference samples [see Fig. 5(b)], in addition to the conductance of the In doping of the sample and has to be subtracted from the measured data.

A constant bulk conductance of 0.19 mS was assumed and subtracted from the sample conductance to obtain the pure contribution of the In dopants. After annealing the corrected conductance corresponds to  $8 \times 10^{12}$   $\text{cm}^{-2}$  electrically active In atoms, meaning that 80% of the implanted In could be activated by the RTA treatment. The changes in conductance measured after H loading and during annealing are now plotted as a sheet concentration of deactivated In atoms in Fig. 12 (open circles) for comparison with the concentration of In-H pairs (solid squares). The two curves agree well within the error bars and always show the same tendency, indicating that every formed or dissociated In-H pair corresponds to a deactivated or reactivated In acceptor, respectively, and therefore justifying the term H passivation.<sup>45</sup>

Of course, a four-point resistivity measurement of a thin implanted layer with mechanical contacts is not the best method to establish a quantitative correlation. Nevertheless, the reproducibility of the data taken for different sample positions under the four-point probe and

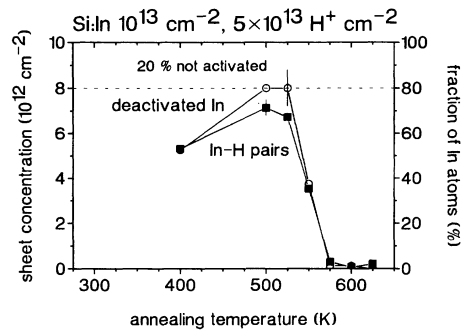


FIG. 12. Comparison of PAC and electrical data of the sample in Fig. 5. The sheet concentration (left scale) of In-H pairs (solid squares) and deactivated In atoms (open circles) is plotted against the annealing temperature. The right scale (fraction of In atoms) refers to all implanted In atoms, of which 20% were not electrically activated by the rapid thermal annealing process.

the reasonable In concentrations obtained after activation, passivation, and reactivation seems quite convincing. As a further check of the assumption made above on the bulk conductance of the sample, it was loaded with a saturation dose of  $10^{15}$   $\text{cm}^{-2}$  after the annealing sequence (Fig. 6). From the measured coupling constant  $\nu_{Q1/-} = 349$  MHz it is concluded that now almost all acceptors are deactivated, because  $\nu_{Q1/-}$  is only observed in Si with low acceptor concentration ( $< 10^{17}$   $\text{cm}^{-3}$ ).<sup>38</sup> The remaining conductance of 0.19 mS is identical to the bulk conductance assumed above and the 78% fraction of In-H pairs corresponds to the initial electrical activation of 80% of the implanted In by the RTA treatment. This result supports the evaluation of the conductance data in Fig. 12.

### C. Formation conditions

H passivation of *p*-type Si can take place during all processes involving the generation of atomic H at the surface or in the bulk of the semiconductor.<sup>11,46</sup> During our studies at <sup>111</sup>In-doped Si, unintentional H passivation was observed under different experimental conditions. In the example of Fig. 7(a) H was obviously driven from the surface or the oxide layer into the bulk by the evaporation of the Pd film and formed In-H pairs. In the second example (b), Cu implantation lead to the predominant formation of In-Cu pairs.<sup>41</sup> But the implantation process produced also some In-H pairs characterized by the coupling constant  $\nu_{Q1/0}$ , in agreement with the B doping of  $1.6 \times 10^{17}$   $\text{cm}^{-3}$  and the temperature of the sample.<sup>38</sup> In contrast to electrical methods, by PAC the differentiation between different passivating species, here Cu and H, is readily possible. The introduced atomic H probably stems from a surface contamination with H<sub>2</sub>O or hydrocarbon molecules which are fragmented by the Cu ions. Similar effects were observed by Seager, Anderson, and Panitz.<sup>7</sup> The strong passivation by air humidity observed in the third sample (c) was obviously supported by the shallow <sup>111</sup>In implantation (60 keV).



Since the H dose is quantitatively controlled if H is implanted, the efficiency of passivation is obtained from Fig. 8(a). For the lowest H dose of  $5 \times 10^{12} \text{ cm}^{-2}$ , 9% of the  $10^{13} \text{ cm}^{-2}$  implanted In atoms formed In-H pairs. This means that about every fifth H atom diffused to an In acceptor and was trapped there, which is a rather high fraction if competitive processes like backscattering (16%), outdiffusion through the near surface (65 Å), and trapping at lattice defects are taken into account. Under the given conditions a dose of  $5 \times 10^{14} \text{ H cm}^{-2}$  is sufficient for a complete passivation of the In acceptors in the sample, visible in the decrease of the sample conductance to the bulk value [see Fig. 8(b)]. At the same time the coupling constant  $\nu_{Q1}$  increases from 335 MHz to its maximum possible value of 349 MHz [Fig. 8(b)], which is characteristic for intrinsic material with the Fermi level near midgap and therefore proves that at least 90% of the In acceptors are electrically inactive.

Compared to the nonquantitative plasma process, the low-energy implantation provides a better defined way of H loading. The implantation energy should be well below 1 keV in order to avoid the production of lattice defects which represent strong competitive traps for H.

#### D. Thermal stability of acceptor-H pairs

For the extraction of dissociation energies, a modeling of H diffusion, taking into account trapping and detrapping of H at acceptor atoms and lattice defects, as was performed by Rizk *et al.*,<sup>48</sup> would be desirable. However, this would not be possible unless the H concentration profiles were known. Therefore the data of the annealing experiments were analyzed assuming that a single jump of the H atom away from the In acceptor is sufficient for a dissociation of the In-H pair. In intrinsic material only doped with radioactive probe atoms, In-H pairs formed by H<sub>2</sub>O loading dissociate sharply at  $T_A = 420 \text{ K}$  [Fig. 10(a)]. If an attempt frequency of  $\nu_0 = 10^{13} \text{ Hz}$  is assumed for the In-H pairs, a dissociation energy  $E_{\text{In-H}} = 1.3 \text{ eV}$  is deduced<sup>34</sup> using Eq. (3), where  $t_A = 10 \text{ min}$  is the isochronal annealing time, and  $f_0$  and  $f(T_A)$  denote the fractions of In-H pairs after H loading and after annealing at  $T_A = 420 \text{ K}$ , respectively:

$$E_{\text{In-H}} = -kT_A \ln \left[ \frac{1}{\nu_0 t_A} \ln \left[ \frac{f_0}{f(T_A)} \right] \right]. \quad (3)$$

This value is an upper limit for the dissociation energy of the In-H pairs because any retrapping of H at the In acceptors would increase the experimentally observed dissociation temperature.

The result obtained for the B-doped samples [Fig. 10(b)], exhibiting first a strong increase of In-H pairs around 380 K and later a much higher dissociation temperature, is explained by the altered equilibrium conditions for the In-H pair concentration. A large amount of B-H pairs is formed near the sample surface during H loading. They dissociate during annealing and release atomic H which can diffuse deeper into the sample where undecorated <sup>111</sup>In acceptors reside. The released H leads to the formation of additional In-H pairs and the fraction

of In-H pairs grows. In addition, the outdiffusion of H from the In-doped region is decelerated by trapping and detrapping processes at the B and In acceptor atoms leading to the strongly increased dissociation temperature. From the temperature around 380 K, where the formation of additional In-H pairs begins,<sup>35</sup> an estimate for the upper limit of the stability of the B-H pairs can be made yielding a dissociation energy of  $E_{\text{B-H}} = 1.1 \text{ eV}$ .

A similar behavior is observed for the Ga-doped samples [Fig. 10(c)] showing an increase of the In-H pairs around 400 K.<sup>47</sup> Thus the dissociation energy of acceptor-H pairs increases from B over Ga to In ranging from 1.1 to 1.3 eV as upper limits. But also in intrinsic samples hydrogenated by a H plasma the dissociation temperature is increased [Fig. 10(d)] compared to loading in H<sub>2</sub>O [Fig. 10(a)]. In this case lattice defects created by the plasma bombardment act as additional H traps in the sample. The intrinsic defects have the same effect as the codoping with B or Ga: They trap and release additional H and slow down the diffusion of H, thereby increasing the apparent stability of the In-H pairs. The data in Fig. 10(a) show that also after low energetic H<sup>+</sup> implantation at 200 eV a slight increase in the dissociation temperature is observed, which is ascribed to the small amount of defects still created by this hydrogenation method. These defects are also visible in the PAC spectra shown in Fig. 4: Lattice defects in different positions near the probe atoms lead to a reduced fraction of probe atoms in an unperturbed surrounding and produce a perturbation in the  $R(t)$  spectra, which is reflected by a reduced value of  $R(t)$  at  $t=0$ . Whereas after H<sub>2</sub>O treatment  $R(t=0)$  is about  $-0.10$ , this value is slightly reduced after H<sup>+</sup> implantation and strongly after H plasma loading.

The effect of high concentrations of acceptor atoms or lattice defects on the observable thermal stability explains why higher dissociation energies have been found after H plasma loading or in highly doped samples. In the review by Pearton, Corbett, and Shi,<sup>5</sup> values of 1.1, 1.6, 1.9, and 2.1 eV are reported for B, Al, Ga, and In, respectively, and Stavola *et al.*<sup>49</sup> found dissociation temperatures of 450, 480, and 580 K for B, Al, and Ga, respectively. In contrast, Zundel and Weber<sup>50</sup> prevented the retrapping of H at the acceptors by removal of H<sup>+</sup> with help of the electric field in a reverse biased Schottky diode in order to ensure pure first-order kinetics of the dissociation process. The dissociation energies were obtained from the development of the active acceptor concentration profiles during annealing, as measured by  $C$ - $V$  profiling. The values of 1.28, 1.44, 1.40, and 1.42 eV for B, Al, Ga, and In, respectively, are in reasonable agreement with the PAC results. Also dissociation energies obtained by modeling of H diffusion profiles in  $p$ -type Si, taking into account the interaction with the acceptor atoms, are similar to our findings.<sup>48</sup>

## VI. SUMMARY

With use of the PAC technique, it was shown that close In-H pairs are formed in Si after loading with H. Four-point resistivity measurements performed in parallel proved that for every formed In-H pair an In acceptor

is electrically deactivated, justifying the use of the term H passivation. In-H pairs are observed following different sample treatments which demonstrates the ease of unintentional contamination of Si with H. With the help of the well-defined low-energy  $H^+$  implantation at 400 K, it is shown that about every fifth H atom introduced is trapped at an acceptor atom. Taking into account strong competitive processes this value represents a high efficiency. For In-H pairs the dissociation energy was directly determined as  $E_{\text{In-H}} \leq 1.3$  eV and indirectly for

B-H pairs as  $E_{\text{B-H}} \leq 1.1$  eV. A systematic tendency of slightly increasing dissociation energy with increasing acceptor size seems to hold for B, Ga, and In.

#### ACKNOWLEDGMENTS

This work has been financially supported by the Deutsche Forschungsgemeinschaft (SFB 306) and the Bundesminister für Forschung und Technologie.

- <sup>1</sup>Chih-Tang Sah, Jack Yaun-Chen Sun, and Joseph Jeng-Tao Tzou, *Appl. Phys. Lett.* **43**, 204 (1983).
- <sup>2</sup>J. I. Pankove, D. E. Carlson, J. E. Berkeyheiser, and R. O. Wance, *Phys. Rev. Lett.* **51**, 2224 (1983).
- <sup>3</sup>J. I. Pankove, R. O. Wance, and J. E. Berkeyheiser, *Appl. Phys. Lett.* **45**, 1100 (1984).
- <sup>4</sup>S. J. Pearton, in *Oxygen, Carbon, Hydrogen and Nitrogen in Crystalline Silicon*, edited by J. C. Mikkelsen, Jr., S. J. Pearton, J. W. Corbett, and S. J. Pennycook, MRS Symposia Proceedings No. 59 (Materials Research Society, Pittsburgh, 1986), p. 457.
- <sup>5</sup>S. J. Pearton, J. W. Corbett, and T. S. Shi, *Appl. Phys. A* **43**, 153 (1987).
- <sup>6</sup>S. T. Pantelides, *Appl. Phys. Lett.* **50**, 995 (1987).
- <sup>7</sup>C. H. Seager, R. A. Anderson, and J. K. G. Panitz, *J. Mater. Res.* **2**, 96 (1987).
- <sup>8</sup>*Hydrogen in Semiconductors*, Vol. 34 of *Semiconductors and Semimetals*, edited by J. I. Pankove and N. M. Johnson (Academic, Boston 1991).
- <sup>9</sup>A. J. Tavendale, A. A. Williams, and S. J. Pearton, *Appl. Phys. Lett.* **48**, 590 (1986).
- <sup>10</sup>A. E. Jaworowski and J. H. Robison, *Mater. Sci. Eng. B* **4**, 51 (1989).
- <sup>11</sup>R. Keller, M. Deicher, W. Pfeiffer, H. Skudlik, D. Steiner, and Th. Wichert, in *Defect Control in Semiconductors*, edited by K. Sumino (North-Holland, Amsterdam, 1990), p. 377.
- <sup>12</sup>N. M. Johnson and M. D. Moyer, *Appl. Phys. Lett.* **46**, 787 (1985).
- <sup>13</sup>J. I. Pankove, P. J. Zanzucchi, C. W. Magee, and G. Lucovsky, *Appl. Phys. Lett.* **46**, 421 (1985).
- <sup>14</sup>N. M. Johnson, *Phys. Rev. B* **31**, 5525 (1985).
- <sup>15</sup>M. Stavola, S. J. Pearton, J. Lopata, and W. C. Dautremont-Smith, *Appl. Phys. Lett.* **50**, 1086 (1987).
- <sup>16</sup>M. Stutzmann, *Phys. Rev. B* **35**, 5921 (1987).
- <sup>17</sup>B. Pajot, A. Chari, M. Aucouturier, M. Astier, and A. Chantre, *Solid State Commun.* **67**, 855 (1988).
- <sup>18</sup>B. Bech Nielsen, J. U. Andersen, and S. J. Pearton, *Phys. Rev. Lett.* **60**, 321 (1988).
- <sup>19</sup>A. D. Marwick, G. S. Oehrlein, J. H. Barrett, and N. M. Johnson, in *Defects in Electronic Materials*, edited by M. Stavola, S. J. Pearton, and G. Davies, MRS Symposia Proceedings No. 104 (Materials Research Society, Pittsburgh, 1988), p. 259.
- <sup>20</sup>Th. Wichert, H. Skudlik, H.-D. Carstanjen, T. Enders, M. Deicher, G. Grübel, R. Keller, L. Song, and M. Stutzmann, in *Defects in Electronic Materials* (Ref. 19), p. 265.
- <sup>21</sup>L. V. C. Assali and J. R. Leite, *Phys. Rev. Lett.* **55**, 403 (1986).
- <sup>22</sup>G. G. DeLeo and W. Beall Fowler, *Phys. Rev. Lett.* **56**, 402 (1986).
- <sup>23</sup>A. Amore Bonapasta, A. Lapicciarella, N. Tomassini, and M. Capizzi, *Phys. Rev. B* **36**, 6228 (1987).
- <sup>24</sup>J. M. Baranowski and J. Tatarikiewicz, *Phys. Rev. B* **35**, 7450 (1987).
- <sup>25</sup>K. J. Chang and D. J. Chadi, *Phys. Rev. Lett.* **60**, 1422 (1988).
- <sup>26</sup>S. K. Estreicher, L. Throckmorton, and D. S. Marynick, *Phys. Rev. B* **39**, 13 241 (1989).
- <sup>27</sup>E. Artacho and F. Ynduráin, *Solid State Commun.* **72**, 393 (1989).
- <sup>28</sup>P. J. H. Denteneer, C. G. Van de Walle, and S. T. Pantelides, *Phys. Rev. B* **39**, 10 809 (1989).
- <sup>29</sup>T. Sasaki and H. Katayama-Yoshida, *J. Phys. Soc. Jpn.* **58**, 1685 (1989).
- <sup>30</sup>A. Chari and M. Aucouturier, *Solid State Commun.* **71**, 105 (1989).
- <sup>31</sup>A. J. Tavendale, D. Alexiev, and A. A. Williams, *Appl. Phys. Lett.* **47**, 316 (1985).
- <sup>32</sup>T. Zundel, A. Mesli, J. C. Muller, and P. Siffert, *Appl. Phys. A* **48**, 31 (1989).
- <sup>33</sup>M. L. W. Thewalt, E. C. Lightowers, and J. I. Pankove, *Appl. Phys. Lett.* **46**, 689 (1985).
- <sup>34</sup>Th. Wichert, H. Skudlik, M. Deicher, G. Grübel, R. Keller, E. Recknagel, and L. Song, *Phys. Rev. Lett.* **59**, 2087 (1987).
- <sup>35</sup>M. Deicher, G. Grübel, R. Keller, E. Recknagel, N. Schulz, H. Skudlik, and Th. Wichert, in *Proceedings of the 15th International Conference on Defects in Semiconductors*, Mater. Sci. Forum **38-41**, edited by G. Ferenczi (Trans Tech, Aedermannsdorf, Switzerland, 1989), p. 1045.
- <sup>36</sup>A. Baurichter, S. Deubler, D. Forkel, M. Gebhard, H. Wolf, and W. Witthuhn, *Mater. Sci. Eng. B* **4**, 281 (1989).
- <sup>37</sup>M. Gebhard, N. Achtziger, A. Baurichter, D. Forkel, B. Vogt, and W. Witthuhn, *Physica B* **170**, 320 (1991).
- <sup>38</sup>H. Skudlik, M. Deicher, R. Keller, R. Magerle, W. Pfeiffer, D. Steiner, E. Recknagel, and Th. Wichert, preceding paper, *Phys. Rev. B* **46**, 2159 (1992).
- <sup>39</sup>Th. Wichert, M. Deicher, G. Grübel, R. Keller, N. Schulz, and H. Skudlik, *Appl. Phys. A* **48**, 59 (1989).
- <sup>40</sup>J. P. Biersack and L. G. Haggmark, *Nucl. Instrum. Methods* **174**, 257 (1980).
- <sup>41</sup>R. Keller, M. Deicher, W. Pfeiffer, H. Skudlik, D. Steiner, and Th. Wichert, *Phys. Rev. Lett.* **65**, 2023 (1990).
- <sup>42</sup>J. C. Mikkelsen, Jr., *Appl. Phys. Lett.* **46**, 882 (1985).
- <sup>43</sup>American Society for Testing and Materials, ASTM F 723-81.
- <sup>44</sup>N. Sclar, *IEEE Trans. Electron Dev.* **ED-24**, 709 (1977).
- <sup>45</sup>H. Skudlik, M. Deicher, R. Keller, R. Magerle, W. Pfeiffer, P. Pross, and Th. Wichert, *Nucl. Instrum. Methods B* **63**, 205 (1992).
- <sup>46</sup>B. Clerjaud, *Physica B* **170**, 383 (1991).
- <sup>47</sup>H. Skudlik, M. Deicher, R. Keller, W. Pfeiffer, D. Steiner, and

Th. Wichert, in *Defect Control in Semiconductors*, edited by K. Sumino (North-Holland, Amsterdam, 1990), p. 413.

<sup>48</sup>R. Rizk, P. de Mierry, D. Ballutaud, M. Aucouturier, and D. Mathiot, *Physica B* **170**, 129 (1991).

<sup>49</sup>M. Stavola, S. J. Pearton, J. Lopata, and W. C. Dautremont-Smith, *Phys. Rev. B* **37**, 8313 (1988).

<sup>50</sup>T. Zundel and J. Weber, *Phys. Rev. B* **39**, 13 549 (1989).